Role of Materials Science and Engineering in Metal Additive Manufacturing

Prabir K. Chaudhury

Education and Consulting LLC, USA

Abstract

Additive Manufacturing or Direct Manufacturing, popularly known as 3D Printing, has become the leading-edge manufacturing technology. Today Metal Additive Manufacturing (MAM) is a reality, not only for prototype fabrication, also for functional parts in all industrial sectors. Design freedom that the AM processes offer has led to design and engineering of new, complex, light-weight structures in all applications. However, in order to realize further and widespread use of metal AM for manufacturing critical components, it is necessary to explore the inherent material freedom in AM. While new metal AM materials are being developed, the role of Materials Science and Engineering (MSE) is becoming more apparent than ever before. This article will highlight the increasing role of Materials Science and Engineering in metal AM, showing the essence of metallurgical principles in realizing full scope of material freedom in metal additive manufacturing. This aper will demonstrate how fundamental MSE principles can be utilized to develop new materials, optimize metal AM and post processing, and their controls that cannot be achieved by conventional manufacturing methods. The examples with new Aluminum AM alloys will be presented, leading to a path of developing advanced and higher performance products for critical applications.

Keywords: Additive manufacturing • Direct manufacturing • Al10SiMg • A357 • Al4MgScZr • Phase diagram • Metastable • Solid solution • Strengthening mechanisms • Lattice parameter • Crystal structure • Coherency

Introduction

Additive Manufacturing or Direct Manufacturing, popularly known as 3D Printing, has become the leading-edge manufacturing technology. Current form of Additive Manufacturing (AM) began its journey utilizing stereolithographic technique [1] to build shapes one layer at a time to rapidly prototype engineered products. These early prototypes were made form photo polymeric materials to bring design to perfection, replicate physical structures, and to check fit and function for engineering products and systems. With advances in the ability to direct, control, and manage high energy sources such as electron beam, laser, plasma, and electric arc to rapidly melt and solidify metals in a thin layer made metal AM possible. Today Metal AM is a reality, not only for prototype fabrication, also for functional parts in all industrial sectors [2]. Because of its inherent advantages to manufacture complex and customizable shapes directly from CAD files without hard tooling, Aerospace and Medical prosthetic industries have embraced metal AM early on [3]. With the advent of topological optimization, the design freedom that AM offers are utilized to reduce weight of metal components and drastically increase buy-to-fly ratio in aerospace industry [4]. Medical prosthetics and implants [5], on the other hand, utilize the ability of metal AM to customize for each patient rapidly at the point of care.

Currently, it is well established that the metal AM is most suitable for production of highly engineered parts with complex geometry, low volume, prototype, custom parts, and parts made from expensive materials [6]. Application of metal AM has now spread in all industrial sectors, especially where advantages of AM can be taken immediately, when just in time manufacturing and lead time reduction are critical. Majority of these parts are functional but non-critical or have large factor of safety because of the limitations in the microstructural and structural deficiencies inherent in metal AM. Similar to the design freedom, metal AM also provides material freedom that has not been sufficiently explored, although major initiatives are in place. Most of the AM metal parts are made from conventional alloys replacing the existing conventionally produced materials. There are very few metal alloys that are additively manufacturable and have the quality or mechanical properties offered by the same alloys when manufactured in conventional processes such as forging. Most of the conventional metal alloys do not respond in the same fashion as in conventional manufacturing because of the rapid melting and solidification they undergo in AM processes. Therefore, the metal AM industry is struggling with new alloy development specific to AM processes. This paper is an attempt to examine the role of Materials Science and Engineering in exercising material freedom in metal AM in order to develop new AM alloys.

Current Metal AM Alloys

In order to examine the role of materials science and engineering in metal AM alloy development, it is necessary to first examine the strategies and principles used currently to develop new AM alloys. Early on metal AM was thought to be an extension or special case of casting and welding processes in which metal alloys are melted and solidified as in metal AM. Therefore, early AM alloy development focused on casting and welding alloy compositions. These alloys were additively manufacturable or printable and exhibited better mechanical properties than cast and weld counterparts because of the structural refinement from very high cooling

rates in metal AM. Wrought compositions exhibited cracking and inferior mechanical properties arising from more than three orders of magnitude faster cooling rates during solidification. The mechanical properties of the wrought materials were not achieved to utilize metal AM for manufacturing critical components. Additional strategy was to select materials that had similar mechanical properties in cast or wrought form as the mechanical properties were tailored based on the post shaping thermal processing. In either approach, the development of AM alloys focused on perfecting processing conditions to develop defect free structure. Many of these AM alloy specifications prefer Hot Isostatic Pressing (HIP) in order to eliminate the porosity and shrinkage defects from AM [7]. Table 1 shows the most popular light weight alloys that have been extensively investigated and recently developed for AM, compiling the data from recent review articles [8,9]. The mechanical properties of these alloys show a large variation because of the large variations in raw material, machines, and processing conditions used in these investigations.

Metal AM alloys	AM Process	Condition	Elastic Modulus	Yield Strength	Tensile Strength	Elongation	Reference
			GPa	MPa	MPa	%	#
Al Alloys							
Al10SiMg	PBF-LB	As Printed	65 - 74	168 - 280	267 - 480	1.0 - 11.0	8,9
		Stress Relieved		215 - 245	295 - 395	10.0 - 14.0	9
Al12Si	PBF-LB	As Printed		211 - 240	357 - 428	3.9 - 5.4	8
A357	PBF-LB	As Printed		232 - 281	424 - 429	4.7 - 10.6	
Al4MgScZr	PBF-LB	As Printed		276 - 287	403 - 427	14 - 17	9
		Heat Treated		520	530	14	
Ti Alloys							
Ti-6Al-4V	PBF - LB	As Printed	91 - 126	736 - 1333	973 - 1407	1.4 - 12.5	8
		Stress Relieved	97 - 123	859 - 1162	932 - 1197	6.5 - 13.1	
		Heat Treated	103 - 117	912 - 1051	986 - 1260	2.6 - 23.0	
		HIPed	106 - 115	831 - 962	907 - 1113	5.0 - 19.0	
	PBF - EB	As Printed	99 - 123	768 - 1147	811 - 1250	2.3 - 16.8	
		HIPed	113 - 121	785 - 894	860 - 990	12.1 - 15.0	
	DED - PLB	As Printed	119	908 - 1124	1015 - 1185	3.0 - 13.0	
		Heat Treated	118	827 - 1000	896 - 1097	1.0 - 16.0	
		HIPed	114 - 118	899 - 946	921 - 1007	11.8 - 19.0	

Table 1. Most investigated Additive Manufacturing metal alloys

As shown in Table 1, there are two types of alloys (Al and Ti) that are based on the two strategies discussed above. In Aluminum alloys, Al10SiMg is the most widely investigated alloy and this along with two other alloys shown, Al12Si and A357 are essentially casting and welding alloys that have been investigated for metal AM. All of these alloys have high Si (7-12 wt.%) to ensure high fluidity during the AM processing. Much of the investigations were focused on the optimizing the process parameters to get nearly 100% densification and various heat treatments to improve ductility in these alloys. No matter how good the powder quality and the printing process are, these alloys yield poor ductility for structural applications in critical applications where wrought AA 6061 is used. Al4MgSc is the only alloy that has been developed specifically for metal AM. This alloy exhibits high strength (>400 MPa) as well as ductility (>10%) in printed as well as heat treated condition. However, because of the very high cost of Sc, even a small addition (0.7%) makes the alloy very expensive for large structural components.

Ti-6Al-4V is the most investigated and utilized metal alloy in AM for both aerospace and medical applications. This and many other alloys such as PH stainless steels and Ni alloys are used in heat treated condition to ensure the optimum size, morphology, and phase constituents in the microstructure for specific properties. These alloys, unlike Aluminum alloys, do not require extensive thermo-mechanical processing to recrystallize fine grains because of their low stacking fault energy. Therefore, the cast and wrought structures exhibit similar properties after heat treatment. In these alloys, particularly in Ti-6Al-4V, the useful microstructure is developed in the solid state as long as the shape can be made by AM processes without defects and porosity. The mechanical properties of this alloy are comparable to cast and wrought version of the same alloy, and loss of ductility mainly arises from the porosity and shrinkage defects which are usually healed by Hot Isostatic Pressing (HIP).

Materials Science and Engineering Principles

Based on the currently available metal AM alloys, it is apparent that the knowledge of materials science and engineering principles can be further utilized for development of metal AM alloys with superior mechanical properties. Conventional metalworking is in practice for hundreds of years, while well understood, utilizes metallurgical principles successfully resulting in thousands of metal alloys for various applications. Comparatively metal AM is new and the difference in the processing conditions and material behavior under these conditions are beginning to be documented. Based on the current data, the differences in the processing conditions and resulting microstructure and basic mechanical properties are compared in Table 2.

Metal Casting and Welding	Metal Additive Manufacturing	Forging and Wrought Metal
Process		
Molten metal is poured in a mold to make the shape	Selectively melted on a substrate with no shaping tooling	Deformed solid metal in a closed or open die set to make the shape
Shaping time is in minutes to hours depending on size	Shaping time is in several hours to weeks depending on size	Shaping time is in seconds or minutes depending on process
Slow cooling from liquid state	Very fast local cooling from liquid and solid state	Slow cooling from solid state
Large melt pool	Very small melt pool	No melting
Structure		
Coarse dendritic microstructure	Very fine dendritic microstructure	Fine Microstructure from recrystallization
Defects are generated in macro- scale but avoided by processing techniques	Defects are generated in meso- and nano scale and controlled by raw material quality and processing parameters	Defects are healed in macro- and meso-scale, generated in micro- scale, and avoided by preforming and chemistry control
Macro- and micro-scale structures define the properties	Meso- and nano-scale structures define the properties	Macro- and micro-scale structures define the properties
Inhomogeneous microstructure	Homogeneous microstructure	Homogeneous microstructure
Properties		
Poor mechanical properties, especially ductility	Better than cast mechanical properties, especially strength	Excellent mechanical properties, both strength and ductility
Properties are isotropic.	Anisotropic properties depending on meso-scale defect alignment along the solidification direction.	Anisotrpic properties are caused by micro-scale defect alignment along the grain flow.

Table 2. Comparison of conventional metal manufacturing processes with AM

As apparent from this and previous table (Table 1), the alloys that are sensitive to quench cracking or distortion or require hot topping or pre-heating during manufacturing are not suitable for metal AM because of the highly localized fast cooling rates. The alloys that are castable and weldable will not provide the mechanical properties unless heat treated to alter the AM microstructure substantially. Therefore, material substitution from conventional manufacturing to AM is not likely to be beneficial, and development of new AM alloys is essential based on the fundamental metallurgical principles. Considering the small melt pool size and very high cooling rates, the phase diagrams, solidification kinetics, crystallinity and crystal structures, and strengthening mechanisms have been discussed in the following for AM metal alloy development.

Phase Diagrams

Binary, Ternary, and multiple element phase diagrams of many alloys have been developed to understand phase transformations under equilibrium conditions. Now with the advent of phase simulation tools such as CALPHAD [10] and JMATPro [11] new, unique, and tailored compositions can be designed based on the equilibrium phase transformations for major conventional processes. Casting and welding processes generally utilize slowest rate practicable to avoid gas porosity, shrinkage cavities, and distortion from thermal gradients. Therefore, the equilibrium phase diagrams are sufficient for alloy development in these cases. In solid state processing such as deformation processing and thermal treatments higher rate of cooling (quenching) is employed to develop desired microstructure and mechanical properties. In these cases, the Time Temperature Transformation (TTT) and Continuous Cooling Transformation (CCT) diagrams are utilized. However, in metal AM processes the cooling rates from molten metal through solid state are very high, in excess of 1000 K/s. At these rates of cooling phase transformation can be suppressed, metastable

phases can develop, and solidification kinetics can change drastically. Only in specialized processes, such as Rapid Solidification Processing (RSP) and Melt Spinning, the solidification rates are as high as those in metal AM.

A recent paper [12] shows the effect of very high rate of cooling on the solidus and liquidus of the equilibrium phase diagram when a binary Al-11.5 at.% Cu hypoeutectic alloy is laser melted and solidified. The as deposited alloy showed a two-phase equiaxed fine microstructure (25 to 35 nm) consisting of Al-Cu solid solution (αAl) with varying composition with 2.3+/-0.7 at.% Cu and Al_2Cu (θ phase) of varying composition with 29.9+/-2.5 at.% Cu. Based on this data, Figure 1 shows the possible solidus and liquidus lines and the effective temperature of complete solidification with no diffusion during solid state cooling under the very high rate of cooling in metal AM.
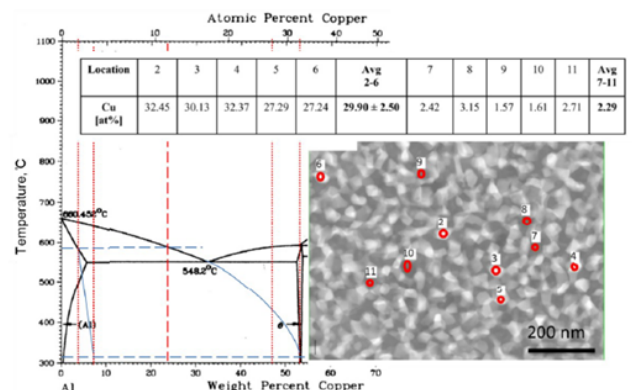

Figure 1. Microstructure and composition of two-phase Al-11.5 at.% Cu alloy in as laser melted and deposited condition and approximate non-equilibrium phase diagram under cooling rates in metal AM processes.

Based on the simplistic analysis shown in Figure 1, the phases present in the as deposited alloy, it is possible to approximately determine the equivalent temperature at which the microstructure developed in the alloy under non-equilibrium cooling. An immediate undercooling of around 300 ºC is apparent in this alloy when laser melted and deposited. While the analysis is simple in binary alloys, ternary alloys and more alloying elements make the phase diagram under non-equilibrium cooling more complex because of the alloy partitioning coefficients and possibility of multiple intermetallic phases, some of which can be metastable. Similar effects of very high cooling rate during solidification and diffusion less solid state transformation are expected in Al-Si, Al-Mg, and other binary eutectic aluminum alloys. In fact Al-Si alloys such as those in Table 1 show a large deviation in chemical composition from those derived from equilibrium phase diagram in the as printed solid microstructure.

Additive Manufacturing of Ti-6Al-4V, on the other hand has little effect on the phase diagram as the solidification temperature is above 1650 ºC with very narrow band of Liquid+beta phase. The beta phase field is very large and extends down to 1000 ºC in this alloy [6]. The high cooling rate in AM affects the meso and macro-scale defects such as porosity and shrinkage. Essentially, effective phase transformations take place in solid state where the beta phase transforms to martensitic alpha prime, or alpha and transformed beta with fine acicular to lamellar microstructure depending on the cooling rate in this region. In Laser Bed Fusion the substrate temperature is much lower than that in Electron Beam Fusion where the powder temperature is kept at around 900 ºC, therefore the microstructure is much finer. The properties in this alloy result from the defect structures during solidification and post-shaping heat treatment.

Solidification

Metal AM is a process of rapid melting and rapid solidification of a very small melt pool. Therefore, solidification from molten liquid is one of the most important steps that needs to be considered in light of type of liquid to solid transformation, chemical composition partitioning, melt pool instability (liquid flow), and shrinkage factors. Two major types of liquid to solid transformation takes place in majority of the engineering metal alloy systems, namely eutectic and peritectic reactions. Most aluminum alloys undergo a eutectic transformation, while the titanium alloys undergo peritectic reaction. Most investigated aluminum alloys shown in Table 1 will be discussed from this perspective.

Four aluminum alloys investigated in AM processes are mainly Al-Si alloys. Mechanical property ranges of three of these are shown in Table 1. All of the alloys are hypoeutectic, but one of them is near eutectic, Al-12%Si [13,14] and the other two of these alloys are hypoeutectic, Al10SiMg [15] and Al7SiMg or A357 [16,17]. Because of rapid cooling in AM, the

microstructure including the phase compositions, and their morphologies are vastly different from casting and welding. In all compositions, the structures in macro-, meso-, and micro-, and nano-scale are very similar as shown in Figure 2 taken directly from the references shown on the Figure 2. Although direct, one to one comparison is not available, all Al-Si hypoeutectic alloys show [18] solidification of fine dendritic Al solid solution (αAl) and eutectic Si at the dendrite boundaries. Al solid solution phase has a columnar morphology and oriented in the direction of rapid heat extraction. While the morphology and the sizes of the two phases are similar in all cases depending on the solidification rate, the main difference is in the composition of the Al solid solution and the eutectic Si phases.
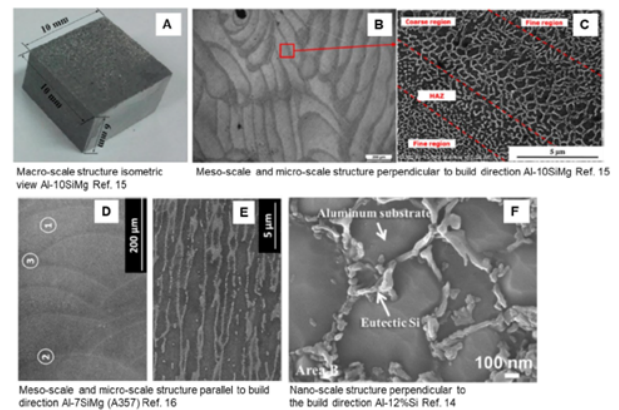

Figure 2. Macro-, Meso-, Micro-, and Nano-scale structures in three hypoeutectic Al-Si alloys taken from references shown with each photograph.

These composition differences are apparently caused mainly by solidification rate and the starting composition of the alloys as explained pictorially in Figure 3. Three alloy compositions, A (Al-12%Si), B (Al-10%Si), and C (Al-7.1%Si) are shown with liquidus composition of AL, BL, and CL with corresponding Solidus compositions of AS, BS, and CS respectively. The solidus and liquidus lines are extended as shown by dash-dot, dash, and dotted lines respectively, based on similar rapid undercooling effects analyzed in Figure 1 for which proportions of solid solution and eutectic phase compositions have been reported [12]. The solidus extends from AS to ASS, BS to BSS, CS to CSS, while the liquidus extends from AL to ASE, BL to BSE, CL to CSE, consistent with the compositions of the Solid Solution (SS) and Solid Eutectic (SE) phases reported [14-18] at room temperature. Large undercooling, lack of diffusion in the solid phase, local solute partitioning at the solid liquid interface, and inhibited mass transport in the liquid phase result in the metastable supersaturated Al solid solution and the eutectic phase with varying Si content as shown in Figure 3 at around 300˚C. The compositions reported are shown in Table 3.

wt.%Si	Liquidus	Solidus	Solid Solution	Eutectic Phase	Ref.
A	12	1.5	11	19	14
B	10	1.3	6.8	14.4	15
C	7.3	1.0	4.5	13	16

Table 3. Metastable phase compositions of Al solid solution and eutectic phases in three hypoeutectic Al-Si alloys
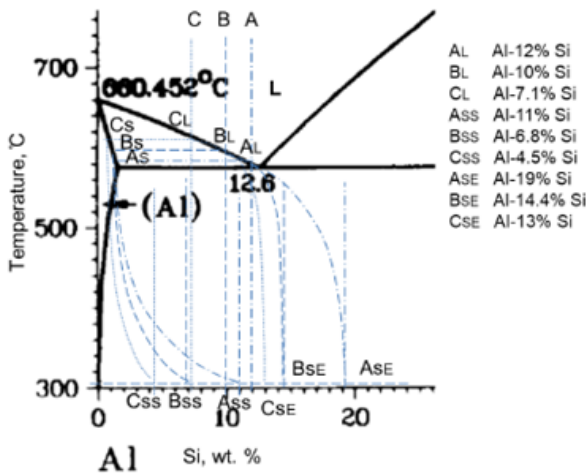
Figure 3. Al-Si partial phase diagram showing metastable phase compositions under rapid cooling during solidification in Powder Bed Fusion with Laser Beam AM processing.

Based on these compositions in the solid state and assuming there is very little, if any, diffusion during cooling from the revised solidus (Figure 3) under non-equilibrium solidification because of very high rate of cooling from the liquidus. In all Al-Si alloys in Table 1, a network of eutectic with fine Si particles in nano scale in as printed condition and fine heterogeneously nucleated αAl matrix provides the strengthening at the expense of ductility of these alloys. Best combination of strength and ductility are observed when the SLM process is optimized to develop fine αAl grains and minimize other defects, such as voids, and shrinkage cavities [17]. In stress relieved and solution treated condition, the Si particles coarsen and spheroidize [16] resulting in higher ductility with substantial loss of strength.

Al4MgScZr alloy, as shown in Table 1 exhibits higher strength and ductility compared to Al-Si alloys, mainly because of the solidification of pro-eutectic nano $Al_3(Sc, Zr)$ phase, increased solute (Mg and Sc) content in metastable αAl, and fine grain structure during high solidification rates in PBF-LB processing. The microstructures in as printed condition shows columnar and equiaxed grains depending on the solidification rate (along the build direction) and location in the melt pool in meso scale [19] similar to all Al alloys. Relatively coarse and very fine grains of αAl are evident on the plane perpendicular to the build direction as shown in Figure 4 [20,21]. Nano-sized, coherent $Al_3(Sc, Zr)$ phase is evident on the αAl grain boundaries and at the grain interior as shown in the Figure 4.

Unlike Al-Si alloys discussed earlier, the Al4MgScZr is an hypereutectic alloy with respect to Sc content (>0.55 at.%) and the first solid to solidify is Al_3Sc ordered L_{12} phase which is coherent with the αAl. With the synergic effect of Zr in this alloy, the pro-eutectic phase is fine, nano-sized $Al_3(Sc_xZr_{1-x})$ which provides the heterogenous nucleation of αAl solid solution with Mg, and remaining Sc and Zr. Because of the large supercooling and high rate of solidification and fixed composition of ordered crystal structure of Al_3Sc, in binary Al-Sc, solidification starts with nucleation of nano-sized Al_3Sc followed by rapid heterogeneous nucleation of the αAl following the non-equilibrium extension of liquidus curve in the binary phase diagram as shown in Figure 5 [22].
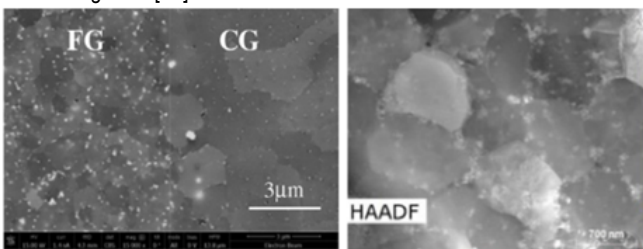

Figure 4. Microstructure of Al4MgScZr alloy in as printed condition showing

intergranular and intragranular $Al_3(Sc,Zr)$ phases in coarse and fine grains of αAl.
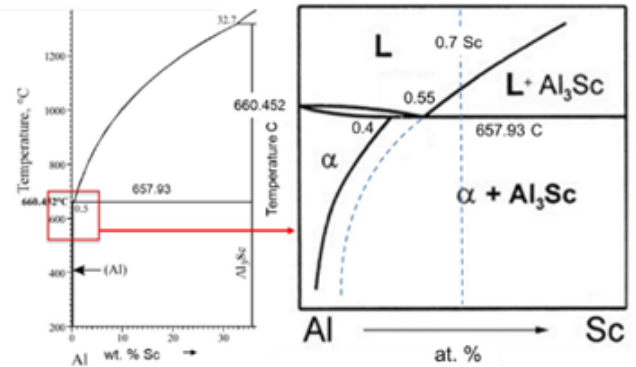

Figure 5. Al-Sc Binary phase diagram showing effect of very high rate of cooling during PBF-LB Additive Manufacturing.

Strengthening Mechanisms

Strengthening mechanisms in metals have been described well in metallurgical engineering text books backed by direct and indirect observations and analyses. All of the mechanisms can be explained in terms of dislocation density and resistance to dislocation motion. In metal additive manufacturing several mechanisms act together based on the alloy chemistry, solidification and phase transformation behavior, and the effect of rapid cooling in a small melt pool. In all Al alloys, under AM processing conditions of high undercooling, very fine (1-10 micron) and supersaturated αAl grains are developed providing both grain boundary and solid solution strengthening. In general, finer the grain size, higher is the number of obstacles for dislocation motion and stronger is the strengthening effect. In solid solution strengthening higher the strain in the lattice due to differences in atomic radius between the solvent and solute, higher is the strengthening. In this case the dislocation motion is obstructed due to the lattice strain and the strengthening effect is weak and dependent on the solute content and the type of solute. In addition, high rate of cooling imposes thermal stresses which result in higher dislocation density in Al alloys which do not recrystallize easily because of their high staking fault energy.

In Al-Si alloys, strengthening also results from the nano-sized Si particles homogeneously distributed in the matrix. Since the Si particles are incoherent with the matrix, they are not deformable and the strengthening effect, while strong, results in loss of ductility. When heat treated to improve ductility, the Si particles coarsen and become scarcely distributed resulting in substantial loss of strength. The properties of all Al-Si alloys as shown in Table 1 vary widely because of the degree of strengthening from supersaturated solid solution, grain size, and Si particle size, quantity, and distribution as well as increased dislocation density. Higher the strength lower is the ductility in all Al-Si alloys making these alloys unsuitable for add critical applications when fabricated by metal AM processes.

In Al4MgSiScZr alloys however, substantial improvement in ductility is observed mainly because of the absence of the incoherent Si particles. In addition to strengthening arising from the grain boundary, solid solution, and dislocation generation from thermal stresses, the $Al_3(Sc, Zr)$ phase in the microstructure plays an important role. Unlike in Al-Si alloys, the $Al_3(Sc, Zr)$ nano particles are coherent with the αAl matrix because of the crystal structure and lattice parameter of this phase. Al_3Sc phase has an ordered cubic (L_{12}) crystal structure with lattice parameter of 0.4103 nm that is very close to that of pure Al, 0.4049 nm (23). Addition of small amount of Zr has a synergic effect, and $Al_3(Sc_xZr_{1-x})$ with x>0.5 retains the L_{12} crystal structure and reduces the lattice parameter up to 0.4092 nm (24) improving the coherency between the two phases. On the other hand, addition of Mg and

presence of Sc and Zr in the metastable supersaturated αAl phase matrix, increases the lattice parameter of the matrix closer to that of the $Al_3(Sc, Zr)$ phase, because of the larger atomic radius of Mg, Sc, and Zr. The nano particles are deformable allowing dislocations to move in this crystal structure with Anti Phase Boundary (APB) strengthening from the ordered nature of the L_{12} crystal structure. Similar to the substantial strengthening in Al-Li alloys with metastable coherent L_{12} ordered crystal structure of Al_3Li [23-25], $Al_3(Sc_xZr_{1-x})$ contribute significantly to the strengthening of Al4MgScZr alloy without the loss of ductility as evident in Table 1.

Conclusion

Fundamentally, both casting and welding utilize equilibrium or near equilibrium cooling conditions during solidification and result in drastically different microstructure in macro, meso, macro and nano scales compared to metal AM. Because of the very high rate of thermal undercooling from liquid to solid in metal AM processes, the equilibrium phase transformations are inhibited. The composition of the solid varies following the extension of solidus and liquidus to a very large drop in temperature. In Al alloys this thermal undercooling is of the order of 300 ºC. The effect of this undercooling is shown to reflect in the composition of the solid phases in Al-Si alloys resulting in supersaturated Al-Si solid solution matrix and finely distributed nano-sized Si particles for increased strength. However, the nano-sized Si particles being incoherent strengthening occurs at the expense ductility. Heat treatments to improve ductility substantially drops the strength as the composition of the αAl matrix change to equilibrium composition with little or no solid solution strengthening, and the Si particles coarsen and distribute scarcely with no precipitation hardening ability.

In Al4MgScZr hypereutectic alloys an ordered L_{12} phase, $Al_3(Sc_xZr_{1-x})$ solidifies first from the liquid and provides nucleation sites for the supersaturated αAl following the liquidus curve on the phase diagram at the highly undercooled temperature. This results in intergranular and intragranular distribution of nano-sized $Al_3(Sc_xZr_{1-x})$ phases in a supersaturated αAl matrix. The L_{12} phase being coherent and ordered, strengthening (Orowan and APB) contribution from the $Al_3(Sc_xZr_{1-x})$ phase has little effect on the ductility drop.

In order to implement metal Additive Manufacturing in critical applications, new applicable materials must be developed using materials science and engineering principles. Phase diagrams and non-equilibrium phase transformations under the high rate of solidification and cooling under AM processing conditions need to be examined. Understanding of the crystal structures, their characteristics, and interaction with dislocations is important to develop new AM materials with enhanced mechanical properties.

References

1. Hull, CW. "Apparatus for production of three-dimensional objects by stereolithography." Patent 4575330 USA (1986).

2. Campbell, I. "Fort Collins, CO." Wohlers Associates Inc (2017).

3. Gibson, I, Rosen DW and Tucker B. "Additive manufacturing technologies rapid prototyping to direct digital manufacturing." New York: Springer (2010).

4. Kamal, M. and Rizza G. "Design for metal additive manufacturing for aerospace applications." [eds.] R Boyer and FH (Sam) Froes. "Additive Manufacturing for the Aerospace Industry." Cambridge, MA: Elsevier (2019): 67-86.

5. Ni, J. "Three dimensional printing of metals for biomedical applications." Materials Today Bio (2019): 1-18.

6. Dutta, B, Babu S and Jared. "B. science, technology and applications of metals in additive manufacturing." Cambridge, MA: Elsevier (2019).

7. Froes, FH, and Dutta B. "The Additive Manufacturing (AM) of titanium alloys." [eds]. M. Qian and F.H. (Sam) Froes. "Titanium Powder Metallurgy Scienece Technology and Applications." Waltham, MA: Elsevier (2015): 447 - 468.

8. Lewandowski, JJ, and Seifi M. "Metal additive manufacturing: A review of mechanical properties." Annual Review of Materials Research (2016): 151 - 186.

9. Aversa, A. "New aluminum alloys specifically designed for laser powder bed fusion." A Review Materials (2019): 1 - 19.

10. CALPHAD Methodology. Thermo calc software. (2020).

11. JMATPRO. Practical software for materials properties. (2020)

12. Bathula, V. "Interface velocity dependent solute trapping and phase selection during rapid solidification of laser melted hypo-eutectic Al-11at.%Cu alloy." Acta Materialia(2020)195: 341 - 357.

13. H. Okamoto, ME Mueller, EM Schlesinger and ASM Handbook. "Al (Aluminum) binary phase diagrams. [eds.] Alloy Phase Diagrams." ASM International (2016)3: 113-139.

14. Yang, Y. "Improved corrosion behavior of ultr-fine grained eutectiv Al-12Si Alloy produced by selective laser melting." Materials and Design (2018) 146: 239-248.

15. Pei, W. "The AlSi10Mg samples produced by selective laser melting: Single track, densification, microstructure and mechanical behavior." Applied Surface Science (2017) 408: 38- 50.

16. Yang, KV. "Effect of heat treatment on the microstructure and anisotropy inmechanical properties of A357 alloy produced by selective laser melting." Materials and Design (2018)154: 275-290.

17. Rao, H. "Influence of processing parameters on aluminum alloy A357 manufactured by selective laser Melting." Materials and Design (2016) 109:334-346.

18. Aboulkhair, NT. "3D printing of Aluminium alloys: Additive Manufacturing of Aluminium alloys using selective laser melting." Progress in Materials Science (2019) 106.

19. Spierings, AB. "Influence of SLM scan-speed on microstructure, precipitation of Al3Sc particles and mechanical properties in Sc- and Zr-modified Al-Mg alloys." Elsevier, Materials and Design (2018) 140: 134-143.

20. Spierings, AB. "Microstructure and mechanical properties of as-processed scandium-modified aluminium using selective laser melting, CIRP Annals - Manufacturing Technology." Materials & Design (2016) 65: 213-216.

21. Spierings, AB. "Microstructural features of Sc- and Zr-modified Al-Mg alloys processed by selective laser melting." Materials & Design (2017)115: 52-63.

22. Davydov, VG. "Scientific principles of making an alloying addition of scandium toaluminium alloys." Materials Science and Engineering (2000) A280: 30-36.

23. DeGraef, M. Crystal structure descriptions, 2nd Edition.

24. Harada, Y and Dunand DC. "Microstructure of Al3Sc with ternary transition-metal additions." Materials Science and Engineereing (2002) 331: 686-695.

25. Nembach, E. "Order strengthening: recent developments, with special reference to aluminium- lithium alloys." Progress in Materials Science (2000) 45: 275-338.